Linear ramps of the mass in the $O(N)$ model: Dynamical transition and quantum noise of excitations

Anna Maraga,[1] Pietro Smacchia,[2] and Alessandro Silva[1,3]

[1]*SISSA, International School for Advanced Studies, via Bonomea 265, 34136 Trieste, Italy*

[2]*Center for Materials Theory, Department of Physics and Astronomy, Rutgers University, Piscataway, New Jersey 08854, USA*

[3]*Abdus Salam ICTP, Strada Costiera 11, 34100 Trieste, Italy*

(Received 4 February 2016; revised manuscript received 1 November 2016; published 16 December 2016)

Nonthermal dynamical critical behavior can arise in isolated quantum systems brought out of equilibrium by a change in time of their parameters. While this phenomenon has been studied in a variety of systems in the case of a sudden quench, we consider here its sensitivity to a change of protocol by considering the experimentally relevant case of a linear ramp in time. Focusing on the $O(N)$ model in the large-N limit, we will show that a dynamical phase transition is always present for all durations of the ramp, and we discuss the crossover between the sudden quench transition and one dominated by the equilibrium quantum critical point. We show that the critical behavior of the statistics of the excitations, signaling the nonthermal nature of the transition, is also robust. An intriguing crossover in the equal-time correlation function, related to an anomalous coarsening, is also discussed.

DOI: 10.1103/PhysRevB.94.245122

I. INTRODUCTION

The nonequilibrium dynamics of isolated quantum many-body systems has been the subject of many theoretical and experimental studies [1–4] in recent years. The interest in this field is mainly motivated by advances in the experimental study of cold atoms trapped in optical lattices [5]. These systems are characterized by a very weak coupling to the external environment, which strongly suppresses dissipative and decoherence effects and allows the observation of the coherent quantum many-body dynamics for quite long time scales. In this context, a series of remarkable experiments led, for example, to the observation of the collapse and revival of a system driven across the Mott-superfluid transition [6,7], the spontaneous symmetry breaking in a quenched spinor Bose-Einstein condensate [8], the absence of thermalization in a one-dimensional Bose gas [9], the phenomenon of prethermalization [10–12], and the light-cone spreading of correlations [13].

Among all the possible ways of taking an isolated quantum system out of equilibrium, the most natural one is to vary in time one of its parameters. A natural goal of any experimental and theoretical characterization of nonequilibrium dynamics is to be able to predict the nature of the steady state attained by a system long after such variation has occurred. While generic systems are expected to approach a thermal state [14–16] even if thermally isolated from the environment, in special cases (i.e., for integrable systems [9,17–21]) relaxation to a nonthermal state described by the generalized Gibbs ensemble (GGE) [22] consistent with all the constants of motion is anticipated. Despite the peculiar nature of integrable systems, signatures of nonthermal behavior may be observed even in nonintegrable ones: the relaxation to a thermal state may indeed involve the approach to a nonthermal quasistationary state (prethermal state) [23–40] on intermediate time scales. Such prethermal states are either expected in low dimensions for systems approximately integrable, as well as in the presence of long-range interactions and in large dimensions close to a mean-field limit. Most importantly, recent literature has shown that such quasistationary states may display dynamical critical behavior. There are two types of dynamical quantum phase transitions in the literature, i.e., criticality in the stationary state attained after a quantum quench and/or singular behavior as a function of time in the so-called Loschmidt amplitude [41]. These two phenomena are related and characterize in a different way the symmetry of quantum trajectories [42]. In the following, we will focus on the first type of criticality. Originally studied for sudden changes of parameters (quenches) in the Hubbard model [43–45], such criticality was later observed in several systems at the mean-field level [46,47] and in field theories [48–51]. While the characterization of these dynamical transitions and their peculiarities as compared to thermal transition is a topic of recent research, it has been recently shown that a simple protocol measuring the quantum noise of excitations produced in a sudden quench can single out their nonequilibrium nature [50].

In general, any dynamical evolution is expected to depend on the particular protocol selected to vary the system parameters. While dynamical transitions were studied for instantaneous variations (sudden quenches), considering more generic procedures, such as a linear ramp, could shed some light on which dynamical features are unaffected by the changes of the protocol and which ones depend on its details (for example, the dependence on its duration). Moreover, the study of generic protocols can be useful for eventual experiments, which typically use linear ramps to prepare and study particular states. In this work, therefore, we address the sensitivity of dynamical transitions to a change of protocol, from a sudden quench to a linear ramp. We focus on the case of an $O(N)$ vector model in the large-N limit, where the model can be solved exactly [52–56], and driving the system out of equilibrium by a linear variation in time of the bare mass, starting in the disordered phase, rather than by a sudden quench. We will show that for this system the dynamical phase transition is robust against changing the protocol and map entirely the crossover between a true dynamical transition and one dominated by the equilibrium quantum critical point as a function of the duration of the ramp τ. In particular, we will discuss analytically how the value of the bare mass at

the dynamical critical point r_c varies as a function of ramp duration, focusing in particular on the two limits of large and small τ. While both critical exponents as well as the behavior of the quantum noise of excitations in a double quench are found to be hardly sensitive to the change of protocol, we observe an intriguing crossover in the equal-time correlation functions displaying anomalous coarsening [57].

The paper is organized as follows. In Sec. II we review the critical properties of the system at equilibrium and in the case of a sudden quench in the bare mass. In Sec. III we study the dynamics of the system when a linear ramp is performed, detecting the dynamical critical point and computing the critical dimensions and exponents. The characterization of the dynamical transition based on the quantum noise of excitations is discussed in Sec. IV, while the case of a linear ramp below the dynamical critical point is studied in Sec. V. In Sec. VI we summarize the results.

II. THE MODEL

In the following, we will focus on the dynamical phase transition in the dynamics of an interacting N component real scalar field $\vec{\phi}$ in d spatial dimensions, described by the Hamiltonian

$$\mathcal{H} = \frac{1}{2}\int d^d x \left[(\vec{\Pi})^2 + (\nabla\vec{\phi})^2 + r_0(\vec{\phi})^2 + \frac{\lambda}{12N}((\vec{\phi})^2)^2 \right], \quad (1)$$

where $\vec{\Pi}$ is the conjugate momentum field. We will be interested in characterizing the dynamical phase transition occurring in the mean-field, $N \to \infty$, limit, where the $O(N)$ vector model is exactly solvable [52]. In this limit and at equilibrium, this system is described by a quadratic theory with an effective mass r, satisfying the self-consistent equation

$$r = r_0 + \frac{\lambda}{6}\int dr \langle\phi^2\rangle, \quad (2)$$

where exploiting the $O(N)$ symmetry of the model, we focused on one of the components of the field $\vec{\phi}$, indicated as ϕ. Using this equation, one may easily see that the system exhibits both a quantum and a thermal phase transition between a paramagnetic phase and an ordered one, characterized by the spontaneous symmetry breaking of the $O(N)$ symmetry [52]. At the critical point, identified by the vanishing of the effective mass r, the bare mass is given by

$$r_0^c = -\frac{\lambda}{12}\int^{\Lambda} \frac{d^d k}{(2\pi)^d}\frac{1}{k}\coth\left(\frac{\beta k}{2}\right), \quad (3)$$

where Λ is the ultraviolet cutoff and β is the inverse temperature. The integral on the right-hand side converges for $d > 2$ ($d > 1$ at zero temperature), setting, therefore, the value for the lower critical dimension. Moreover, one can compute the critical exponent ν describing the divergent behavior of the correlation length $\xi \sim r^{-1}$ close to the critical point, i.e., $\xi \sim (\delta r_0)^{-\nu}$, with $\delta r_0 = r_0 - r_0^c$. At $T = 0$, one finds $\nu = 1/(d-1)$ for $1 < d < 3$ and $\nu = 1/2$ for $d \geqslant 3$, which is therefore the upper critical dimension of the quantum phase transition. In the finite-temperature case, one gets instead $\nu = 1/(d-2)$ for $2 < d < 4$ and $\nu = 1/2$ for $d \geqslant 4$, which implies that $d = 4$ is the upper critical dimension for the thermal transition.

Focusing now on the dynamics, it has been shown numerically [49,50,58,59] that this model can undergo a dynamical phase transition after a sudden quench in the bare mass, i.e., suddenly changing its value from $r_{0,i}$ to $r_{0,f}$ (we focus here on the case of a sudden quench starting from the ground state in the paramagnetic phase). The time-dependent effective mass [satisfying Eq. (2) with a time-dependent correlation function $\langle\phi^2(t)\rangle$ dictating the self-consistency] is seen to oscillate and then relax to a well-defined value at large times. The stationary value $r^\star$ of the effective mass can be predicted efficiently via an ansatz [58] (see below) based on the replacement of the equal-time correlation function $\langle\phi^2(t)\rangle$ in Eq. (2) with the stationary, time-averaged part of corresponding post-quench correlator for a free theory ($\lambda = 0$) with the initial and final values of the mass set equal to r_i and $r^\star$. The dynamical critical point is therefore reached provided the final bare mass satisfies the relation

$$r_{0,f}^c = -\frac{\lambda}{24}\int^{\Lambda} \frac{d^d k}{(2\pi)^d}\frac{2k^2 + r_i}{k^2\sqrt{k^2 + r_i}}, \quad (4)$$

where r_i indicates the effective mass before the sudden quench.

From this equation, one obtains that the lower critical dimension for the dynamical transition is $d = 2$, and that the value of the bare mass at the dynamical critical point is always smaller than the one at the quantum critical point r_0^c. As in the equilibrium case, we denote with ξ^* the correlation length in the stationary state and with ν^* the exponent describing its divergence close to the dynamical critical point. We find that $\nu^* = 1/(d-2)$ for $2 < d < 4$ and $\nu^* = 1/2$ for $d \geqslant 4$, which is the upper critical dimension. The fact that these critical exponents are similar to those of a thermal transition at equilibrium suggests that the two might be analogous [50,59]. Indeed, one could imagine that fixing r_0^f in the equilibrium ordered phase and increasing r_0^i from r_0^f to higher values amounts to increase the energy density injected by the sudden quench into the system. This could be seen as equivalent to moving from low to high temperatures in the corresponding equilibrium phase diagram, in which case a thermal phase transition would sooner or later be crossed. Notice, however, that, despite the analogies, the distribution of quasiparticles after a sudden quench in the $N \to +\infty$ limit *is not* thermal. Moreover, the difference between the two cases becomes apparent if one studies the quantum noise of excitations produced close to a dynamical transition, since, unlike the equilibrium case, in the dynamical one the fluctuations in the number of excitations are very sensitive to how close one is to a dynamical critical point [50].

III. DYNAMICS AND DYNAMICAL CRITICAL PROPERTIES FOR A LINEAR RAMP

In this paper, we address the robustness of the scenario above with respect to a change of protocol from a sudden quench to a linear ramp of the bare mass. The system is initially prepared in the ground state of the disordered phase ($r_{0,i} > r_0^c$), then the bare mass is linearly decreased to a final value $r_{0,f}$ according to the following protocol: $r_0(t) = r_{0,i}$ for $t < 0$, $r_0(t) = r_{0,i} + (r_{0,f} - r_{0,i})t/\tau$ for $0 \leqslant t \leqslant \tau$, and $r_0(t) = r_{0,f}$ for $t > \tau$.

Let us start setting up the formalism to study the dynamics in the $N \to +\infty$ limit [53,54]. The system is again described by an effective quadratic Hamiltonian with a time-dependent effective mass $r(t)$. Exploiting the $O(N)$ symmetry of the model, we can focus on only one component of the field. Passing to Fourier space, we may write

$$\mathcal{H}_{\rm eff}(t) = \frac{1}{2}\int^{\Lambda} \frac{d^d k}{(2\pi)^d}\left[\Pi_{\mathbf{k}}(t)\Pi_{-\mathbf{k}}(t) + \omega_k^2(t)\phi_{\mathbf{k}}(t)\phi_{-\mathbf{k}}(t)\right], \tag{5}$$

where $\omega_k(t) = \sqrt{k^2 + r(t)}$, and

$$r(t) = r_0(t) + \frac{\lambda}{6}\int^{\Lambda} \frac{d^d k}{(2\pi)^d}\langle\phi_{\mathbf{k}}(t)\phi_{-\mathbf{k}}(t)\rangle. \tag{6}$$

Let us now expand the field in the Heisenberg representation as

$$\phi_{\mathbf{k}}(t) = f_k(t)a_{\mathbf{k}} + f_k^{\star}(t)a_{-\mathbf{k}}^{\dagger}, \tag{7}$$

where $a_{\mathbf{k}}$ and $a_{\mathbf{k}}^{\dagger}$ diagonalize the initial Hamiltonian (5) at $t = 0$, and $f_k(t)$ is a complex amplitude. Imposing the Heisenberg equations of motion for $\phi_{\mathbf{k}}(t)$, we derive the equation for the evolution of the mode function $f_k(t)$,

$$\ddot{f}_k(t) + [k^2 + r(t)]f_k(t) = 0, \tag{8a}$$

where

$$r(t) = r_0(t) + \frac{\lambda}{6}\int^{\Lambda} \frac{d^d k}{(2\pi)^d}|f_k(t)|^2 \tag{8b}$$

and the initial conditions are $f_k(0) = 1/\sqrt{2\omega_k(0)}$ and $\dot{f}_k(0) = -i\sqrt{\omega_k(0)/2}$, with $\omega_k(0) = \sqrt{k^2 + r_i}$.

These equations have the same form as those obtained for a sudden quench, with the only difference that r_0 is now not a constant but a linear function of time. In particular, Eq. (8) can be solved analytically for a linear ramp in the special case of $\lambda = 0$ (see Appendix A). For any finite λ, one instead has to resort to numerical integration. Varying the duration of the ramp and the value of the final bare mass, the system is found to display again a dynamical phase transition: as shown in Fig. 1, long after the end of the ramp, the effective mass $r(t)$ is seen to relax to a stationary value, which is positive up to a certain τ-dependent dynamical critical value $r_{0,f}^c(\tau)$, and it vanishes for $r_{0,f} \leqslant r_{0,f}^c(\tau)$.

Stationary state and dynamical criticality

Let us now characterize thoroughly the dynamical phase transition as a function of initial and final parameters and ramp duration τ. First of all, it is important, as in the case of a sudden quench, to be able to predict analytically the stationary value of the effective mass r^*. To achieve this goal, we introduced an ansatz for the stationary effective mass inspired by the one used before for a sudden quench [50,58]: we assume the stationary part of the equal-time Green's function $\langle\phi_{\mathbf{k}}(t)\phi_{-\mathbf{k}}(t)\rangle = |f_k(t)|^2$ to be equal to the noninteracting ($\lambda = 0$) one, with the bare masses replaced by the renormalized ones, namely $r_{0,i} \to r_i$ [which can be calculated with Eq. (8) with $t < 0$] and $r_{0,f} \to r^*$ (see Appendix A). We therefore

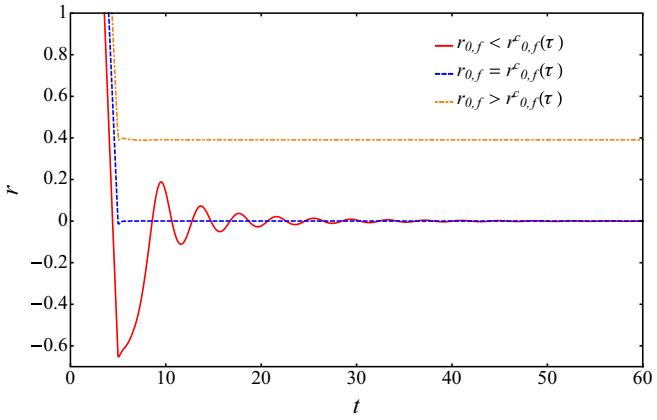

FIG. 1. Time evolution of the effective mass $r(t)$ for ramps of duration $\tau = 5$, initial bare mass $r_{0,i=5}$ in $d = 3$, and interaction strength $\lambda = 15$. Final values of the bare mass below, at, and above the dynamical critical point are shown.

obtain the following self-consistent equation for r^*:

$$r^* = r_{0,f} + \frac{\lambda}{12}\int^{\Lambda} \frac{d^d k}{(2\pi)^d}\left[|f_k^0(r^*,\tilde{\tau})|^2 + \frac{|\dot{f}_k^0(r^*,\tilde{\tau})|^2}{k^2 + r^*}\right], \tag{9}$$

where f_k^0 denotes the mode function that solves Eq. (8a) for $\lambda = 0$ and $r(t) = r^{\star}$ at time τ [see Eqs. (A6) and (A7)]. According to this ansatz, we can identify the value of the bare mass at the dynamical critical point for which r^* vanishes as

$$r_{0,f}^c(\tau) = -\frac{\lambda}{12}\int^{\Lambda} \frac{d^d k}{(2\pi)^d}\left[|f_k^0(0,\tilde{\tau})|^2 + \frac{|\dot{f}_k^0(0,\tilde{\tau})|^2}{k^2}\right]. \tag{10}$$

The mere fact that the stationary state can be described by an ansatz such as Eq. (9) allows us to deduce many of the properties of the dynamical phase transition. Note, however, that in order to obtain the correct stationary value for $r_{0,f} \geqslant r_{0,f}^c(\tau)$, we had to renormalize the ramp duration τ to an effective value $\tilde{\tau}$ in Eq. (9). Such a renormalized value increases as τ does (see the discussion below). Notice that making $\tilde{\tau}$ an adjustable parameter does not allow us to fit any function, but it has a clear physical significance. Indeed, by rewriting Eq. (9) as

$$r^{\star} - r_{0,f} = I(\tilde{\tau}), \tag{11}$$

with

$$I(\tilde{\tau}) = \frac{\lambda}{12}\int^{\Lambda} \frac{d^d k}{(2\pi)^d}\left[|f_k^0(r^*,\tilde{\tau})|^2 + \frac{|\dot{f}_k^0(r^*,\tilde{\tau})|^2}{k^2 + r^*}\right], \tag{12}$$

the above equation determines the effective ramp duration τ given the final bare mass $r_{0,f}$ and the observed asymptotic effective mass $r^{\star}$. The function $I(\tilde{\tau})$ is an increasing function of $\tilde{\tau}$, with the limiting values

$$I(0) = \frac{\lambda}{48\Pi^2}\int_0^{\Lambda} dk\, k^2 \frac{2k^2 + r_i + r^{\star}}{(k^2 + r^{\star})\sqrt{k^2 + r_i}},$$
$$I(\tilde{\tau} \to \infty) = \frac{\lambda}{24\Pi^2}\int_0^{\Lambda} dk \frac{k^2}{\sqrt{k^2 + r^{\star}}}. \tag{13}$$

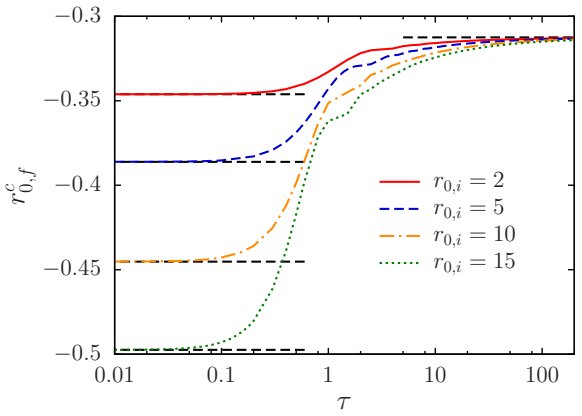

FIG. 2. Value of the mass at the dynamical critical point $r^c_{0,f}(\tau)$ as a function of the ramp duration τ in $d = 3$. Different values of the initial bare mass $r_{0,i}$ are shown, while the interaction is $\lambda = 15$. Horizontal black dashed lines indicate the value of the bare mass at the dynamical critical point for a sudden quench ($\tau \to 0$) and that at the quantum critical point for the equilibrium case ($\tau \to \infty$).

Both of these values are positive and finite, so the ansatz can work only if the difference $r^\star - r_{0,f}$ is always between these two limits and cannot fit any value. There is, of course, no guarantee that this would always be the case, therefore the fact that the ansatz works is certainly not trivial.

Let us now establish the lower critical dimension of the dynamical transition by analyzing the behavior for low momenta of the integrand of Eq. (10) (see Appendix B). Inspection of Eq. (10) shows that for every finite τ, the modes that contribute the most to the integral on the right-hand side are those with $k \ll \min[(r_i/\tilde{\tau})^{1/3}, \sqrt{r_i}]$, where both $|f^0_k(0,\tilde{\tau})|^2$ and $|\dot{f}^0_k(0,\tilde{\tau})|^2$ go to a constant, making the integrand behave as $1/k^2$. This implies that the value of the bare mass at the dynamical critical point $r^c_{0,f}(\tau)$ is finite for $d > 2$, $d = 2$ being the lower critical dimension for every finite τ. We observe that as τ increases, the region considered above shrinks. Moreover, as τ gets larger and larger, the region of intermediate asymptotics $(r_i/\tilde{\tau})^{1/3} \ll k \ll \sqrt{r_i}$, where $|f^0_k(0,\tilde{\tau})|^2 \sim 1/k$ and $|\dot{f}^0_k(0,\tilde{\tau})|^2 \sim k$, becomes more and more important. When τ becomes infinite, this asymptotics dominates and the lower critical dimension becomes $d = 1$, recovering the result of the quantum transition. As shown in Fig. 2, the values of $r^c_{0,f}(\tau)$ interpolate between the value of the bare mass at the dynamical critical point for a sudden quench, corresponding to $\tau \to 0$, and that at the quantum critical point at equilibrium, in the limit of large τ.

It is now important to study the dependence of $\tilde{\tau}$ on τ. Equation (9) provides the correct stationary value of the effective mass provided the parameter $\tilde{\tau}$ is adjusted, a task that can be accomplished numerically. In particular, once the dynamical critical point has been identified, we can compute *a posteriori* the effective ramp duration $\tilde{\tau}$ at criticality using Eq. (10). Analyzing the behavior of $\tilde{\tau}$ as a function of the true ramp duration τ at the critical point and for $r_{0,i}$ and λ fixed, it turns out that in the limits of small and large τ these two quantities have a linear relation, as can be seen in Fig. 3. Moreover, varying the value of the initial bare mass $r_{0,i}$ (but keeping λ fixed), the different $\tilde{\tau}(\tau)$ collapse on the same line,

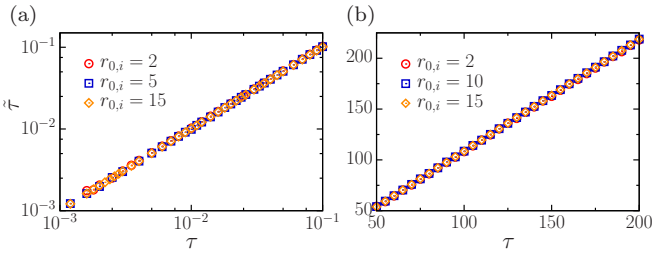

FIG. 3. Effective ramp duration $\tilde{\tau}$ as a function of the true ramp duration τ at the dynamical critical point in $d = 3$ for small (a) and large (b) τ. Different values of the initial bare mass $r_{0,i}$ are shown, while the interaction is $\lambda = 15$.

for large and small τ. We may therefore use the ansatz (10) to analytically study how the dynamical critical value depends on τ in two limiting cases, for $\tau \to \infty$ (adiabatic switching) and $\tau \to 0$ (sudden quench). Note that the linear relation between τ and $\tilde{\tau}$ is not valid for intermediate values of τ, as can be seen from Fig. 4. There we can see that oscillations are present in the intermediate regime, and different values of the initial bare mass r_{0i} do not collapse one on each other. Moreover, it is worth noting that the two linear relationships valid at small and large τ are different from each other.

Our ansatz, together with the linear relation between τ and $\tilde{\tau}$ at large τ and small τ, will now allow us to map entirely analytically the crossover between sudden quenches and linear ramps. Let us start with large τ and employ Eq. (10) to study the crossover in Fig. 2. We will use in particular the exact solutions for the noninteracting mode functions $f^0_k(t)$ expressed in terms of Airy functions (see Appendix A). Employing the asymptotic expansion of the Airy functions for large and negative arguments (see Appendix B), for $\tilde{\tau} \gg 1/\sqrt{r_i}$

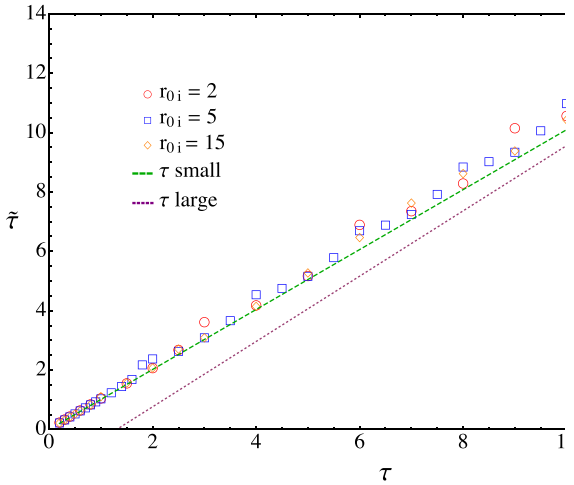

FIG. 4. Effective ramp duration $\tilde{\tau}$ as a function of the true ramp duration τ at the dynamical critical point in $d = 3$ for intermediate τ. Different values of the initial bare mass $r_{0,i}$ are shown, while the interaction is $\lambda = 15$. The dashed green line and the dotted purple line represent the linear relation between the quantities that are valid at small and large τ, respectively.

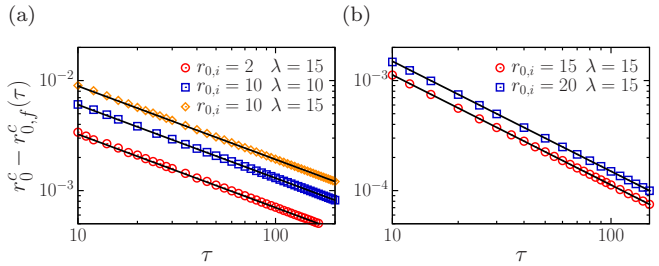

FIG. 5. Difference between the value of the bare mass at the quantum critical point r_0^c and that at the dynamical critical point $r_{0,f}^c(\tau)$ for large ramp duration τ in $d = 3$ (a) and $d = 4$ (b). Different values of the interaction λ and of the initial bare mass $r_{0,i}$ are shown. Black lines are proportional to $\tau^{-2/3}$ (a) and to τ^{-1} (b).

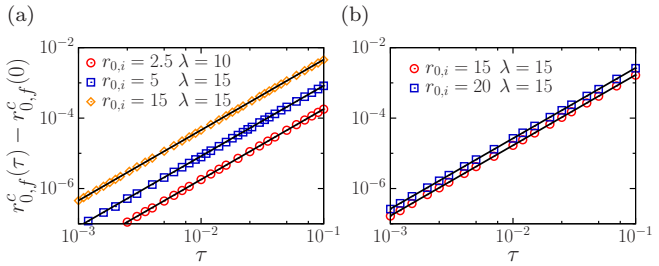

FIG. 6. Difference between the value of the bare mass at the dynamical critical point for a ramp, $r_{0,f}^c(\tau)$, and for a sudden quench, $r_{0,f}^c(0)$, for small ramp duration τ in $d = 3$ (a) and $d = 4$ (b). Different values of the interaction λ and of the initial bare mass $r_{0,i}$ are shown. Black lines are proportional to τ^2.

Eq. (10) reads

$$r_{0,f}^c(\tau) \simeq -\frac{\lambda}{12}\frac{\Omega(d)}{(2\pi)^d}[\mathcal{I}_1(d) + \mathcal{I}_2(d)], \tag{14}$$

where $\Omega(d)$ is the solid angle in d dimension, and

$$\mathcal{I}_1(d) = \frac{\pi}{4}\Lambda^d\left(\frac{\tilde{\tau}}{r_i}\right)^{1/3}\int_0^1 dz\, z^{\frac{d-2}{2}} \times\left[\mathrm{Ai}^2\left(-\frac{\Lambda^2\tilde{\tau}^{2/3}}{r_i^{2/3}}z\right) + \mathrm{Bi}^2\left(-\frac{\Lambda^2\tilde{\tau}^{2/3}}{r_i^{2/3}}z\right)\right], \tag{15a}$$

$$\mathcal{I}_2(d) = \frac{\pi}{4}\Lambda^{d-2}\left(\frac{r_i}{\tilde{\tau}}\right)^{1/3}\int_0^1 dz\, z^{\frac{d-4}{2}} \times\left[\mathrm{Ai}'^2\left(-\frac{\Lambda^2\tilde{\tau}^{2/3}}{r_i^{2/3}}z\right) + \mathrm{Bi}'^2\left(-\frac{\Lambda^2\tilde{\tau}^{2/3}}{r_i^{2/3}}z\right)\right], \tag{15b}$$

where we introduced the dimensionless variable $z = k^2/\Lambda^2$.

Integrals (15) can be computed exactly both in $d = 3$ and 4 (see Appendix C). We find that the asymptotic value of the bare mass at the dynamical critical point for large τ and $d = 3$ is

$$r_{0,f}^c(\tau) = r_0^c + \frac{\lambda\,\Gamma(-1/3)}{2^{17/3}\times 3^{7/3}\,\pi^2}\left(\frac{r_i}{\tilde{\tau}}\right)^{2/3} + O\left(\frac{r_i^{4/3}}{\Lambda^4\tilde{\tau}^{4/3}}\right), \tag{16}$$

while for $d = 4$ it is

$$r_{0,f}^c(\tau) = r_0^c - \frac{\lambda}{1152\sqrt{3}\,\pi^2}\left(\frac{r_i}{\tilde{\tau}}\right) + O\left(\frac{r_i^2}{\Lambda^6\tilde{\tau}^2}\right), \tag{17}$$

where r_0^c is the quantum critical point at equilibrium [see Eq. (3)]. In both cases, $r_{0,f}^c$ is smaller than the equilibrium critical point.

Since for large τ the relation between $\tilde{\tau}$ and τ is linear at the critical point, we conclude that the value of the bare mass at the dynamical critical point approaches the quantum critical value as $\tau^{-2/3}$ for $d = 3$ and as τ^{-1} for $d = 4$. We verified these scalings numerically by linearly fitting the relation between $\tilde{\tau}$ and τ for large τ and replacing the result in Eqs. (16) and (17), getting an excellent agreement with numerical data, as shown in Fig. 5.

Let us now consider the fate of the dynamical critical point in the limit of small τ. By using the asymptotic expansion of the Airy functions for small arguments (see Appendix B), we have that

$$\left|f_k^0(0,\tilde{\tau})\right|^2 \simeq \frac{1}{2\sqrt{k^2+r_i}} + \frac{r_i}{6\sqrt{k^2+r_i}}\,\tilde{\tau}^2, \tag{18}$$

$$\left|\dot{f}_k^0(0,\tilde{\tau})\right|^2 \simeq \frac{\sqrt{k^2+r_i}}{2} - \frac{4k^2r_i + r_i^2}{24\sqrt{k^2+r_i}}\,\tilde{\tau}^2. \tag{19}$$

Inserting these expressions in Eq. (10), we obtain

$$r_{0,f}^c(\tau) \simeq r_{0,f}^c(0) + \frac{\lambda}{12}\,\tilde{\tau}^2\int^\Lambda \frac{d^dk}{(2\pi)^d}\frac{r_i^2}{24k^2\sqrt{k^2+r_i}}, \tag{20}$$

where $r_{0,f}^c(0)$ is the value of the bare mass at the dynamical critical point for a sudden quench [see Eq. (4)].

Since at criticality $\tilde{\tau} \sim \tau$ for small τ, we conclude that the value of the bare mass at the dynamical critical point departs from the sudden quench value as τ^2, both in $d = 3$ and 4. This is confirmed by numerical data (Fig. 6).

We are now ready to compute the critical exponent ν^*, describing the divergence of the correlation length ξ^* in the stationary state close to the dynamical critical point, i.e., $\xi^* \sim [\delta r_{0,f}(\tau)]^{-\nu^*}$, with $\delta r_{0,f}(\tau) = r_{0,f} - r_{0,f}^c(\tau)$ combining Eqs. (9) and (10). As shown in detail in Appendix B, for $2 < d < 4$ the stationary value of the effective mass at the leading order scales as $r^* \sim [\delta r_{0,f}(\tau)]^{\frac{2}{d-2}}$, while for $d \geqslant 4$ the scaling becomes linear, i.e., $r^* \sim \delta r_{0,f}(\tau)$. Since the theory is Gaussian, $(\xi^*)^{-1} \sim \sqrt{r^*}$. We conclude that

$$\begin{aligned} &\nu^* = 1/(d-2) \quad &&\text{for } 2 < d < 4,\\ &\nu^* = 1/2 &&\text{for } d \geqslant 4, \end{aligned} \tag{21}$$

$d = 4$ being the upper critical dimension. Figure 7 shows that numerical results for $d = 3$ and 4 agree with this prediction. We note that for $d = 3$ [Fig. 7(a)] numerical data follow the relation $r^* \sim [\delta r_{0,f}(\tau)]^2$ for sufficiently small values of r^* and then depart from this scaling, eventually approaching a linear relation for larger r^*, indicating a crossover between $d = 3$ critical and mean-field behavior.

As in the case of a sudden quench, the critical dimensions and the critical exponent turn out to be the same as the thermal one, even though we are dealing here with the unitary dynamics of a pure state and not with a mixed state. Similar behavior is observed in other models, such as the infinite-range Ising model (Lipkin model) [47,60]. Only when τ is strictly infinite do we eventually recover the results of the quantum transition.

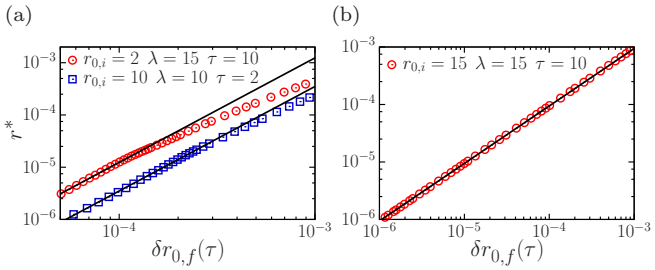

FIG. 7. Stationary value of the mass as a function of the distance from the dynamical critical point in $d = 3$ (a) and $d = 4$ (b). Black lines are quadratic (a) and linear (b) fits.

Notice that despite the fact that such exponents are identical to the thermal ones in the $N \to \infty$ limit, we cannot rule out that the $1/N$ corrections will be different. This issue is left for future studies.

IV. QUANTUM NOISE OF EXCITATIONS

To complete our characterization of the crossover in the dynamical transition, we study the quantum noise of excitations produced by the ramp of the bare mass, generalizing the approach proposed in Ref. [50]. As in the case of a sudden quench, we will show that the growth in time of the fluctuations in the number of excitations bears strong signatures of the dynamical transition.

The protocol we will study is the following: after the end of the ramp, we let the system evolve for a certain waiting time, after which we suddenly quench the bare mass back to its initial value $r_{0,i}$. The number of excitations generated in this process is a fluctuating quantity characterized by a certain probability distribution related to the operator

$$\hat{\mathcal{N}} = \int^{\Lambda} \frac{d^d k}{(2\pi)^d}\, a^{\dagger}_{\mathbf{k}} a_{\mathbf{k}}. \tag{22}$$

An equivalent and more convenient description can be given in terms of the moment-generating function

$$G(s,t) = \langle \psi(t)|\, e^{-s\hat{\mathcal{N}}}\, |\psi(t)\rangle, \tag{23}$$

where $|\psi(t)\rangle = U(t)\,|0\rangle$ is the evolved state at time t, and $|0\rangle$ indicates the initial ground state. The explicit derivation of $G(s,t)$ is presented in Appendix D. In particular, we obtain

$$\ln G(s,t) = -\frac{V}{2}\int^{\Lambda} \frac{d^d k}{(2\pi)^d}\, \ln[1 + \rho_k(t)(1 - e^{-2s})], \tag{24}$$

where

$$\rho_k(t) = \frac{1}{2}\left[\omega_k(0)|f_k(t)|^2 + \frac{|\dot{f}_k(t)|^2}{\omega_k(0)} - 1\right] \tag{25}$$

and $V = L^d$, L being the linear size of the system. Notice that this quantity is exactly the number of excitations per mode studied in the context of inflation and preheating dynamics [55,56].

The dynamical critical properties of the system can be studied by analyzing the cumulants of the distribution of excitations, defined as

$$C_n(t) = (-1)^n \frac{\partial^n}{\partial s^n} \ln G(s,t)\bigg|_{s=0}. \tag{26}$$

In the following, we will focus on the first two cumulants, i.e., the average $\overline{\mathcal{N}}(t)$ and the variance $\sigma^2(t)$, in $d = 3$ and 4, and we numerically study their time dependence, trying to distinguish qualitatively different behaviors for different values of the bare mass at the end of the ramp. Their explicit expressions in terms of $\rho_k(t)$ are

$$\frac{\overline{\mathcal{N}}(t)}{V} = \int^{\Lambda} \frac{d^d k}{(2\pi)^d}\, \rho_k(t), \tag{27}$$

$$\frac{\sigma^2(t)}{V} = \int^{\Lambda} \frac{d^d k}{(2\pi)^d}\, 2\rho_k(t)[1 + \rho_k(t)]. \tag{28}$$

For large times, the average number of excitations relaxes to a finite value for every value of $r_{0,f}$, both in $d = 3$ and 4. Remarkably, the variance per unit volume displays a nontrivial behavior at large times, depending on the final value of the bare mass $r_{0,f}$. For ramps ending above the dynamical critical point, i.e., $r_{0,f} > r^c_{0,f}(\tau)$, the variance saturates to a finite value, both in $d = 3$ and in $d = 4$ [Figs. 8(a) and 8(d)]. For $r_{0,f} < r^c_{0,f}(\tau)$, the variance increases algebraically: for $d = 3$ it scales as $\sigma^2 \sim t$ [Fig. 8(c)], while for $d = 4$ it scales as $\sigma^2 \sim t^2$ [Fig. 8(f)]. Finally, for ramps at the critical point, i.e., $r_{0,f} = r^c_{0,f}(\tau)$, the variance grows logarithmically in time, both in $d = 3$ and in $d = 4$ [Figs. 8(b) and 8(e)].

We note that this behavior is the same as that observed in the case of a sudden quench [50], showing that the critical scaling of the variance appears to be unaffected by the change of the protocol.

V. LINEAR RAMP BELOW THE DYNAMICAL CRITICAL POINT

An interesting signature of the crossover between sudden quench and slow ramp is observed by focusing on ramps below the dynamical critical point. It has been shown [57] that performing a sudden quench below the dynamical critical point induces the emergence of a scaling form in the correlation functions associated with coarsening dynamics with an exponent characterizing these functions differing from the one expected in the usual classical coarsening. The reason for this discrepancy between quantum and classical systems has been unclear up to now. In particular, in the case of standard coarsening, one would expect the correlation function to scale as $G(r,t) = G[r/L(t)]$ and $G(k,t) = L(t)^d G[kL(t)]$. As shown in Ref. [57] and discussed below [see Eq. (30)], this is not consistent with what was obtained in the case of a quantum quench. To see this in the most general case, let us now investigate how this behavior is affected by a linear ramp in the bare mass. Toward that end, we consider the equal-time two-point correlation function $\langle \phi_{\mathbf{k}}(t)\phi_{-\mathbf{k}}(t)\rangle = |f_k(t)|^2$ and its Fourier transform $\langle \phi(\mathbf{x},t)\phi(\mathbf{y},t)\rangle$ in $d = 3$ and 4.

As a consequence of the ramp protocol, the dependence of $\langle \phi_{\mathbf{k}}(t)\phi_{-\mathbf{k}}(t)\rangle$ on momentum k displays two different regimes. Right at the end of the ramp [Figs. 9(a) and 9(d)], we note that it exhibits the following scaling form:

$$\langle \phi_{\mathbf{k}}(\tau)\phi_{-\mathbf{k}}(\tau)\rangle = \tau^d \mathcal{F}_d(k\tau), \tag{29}$$

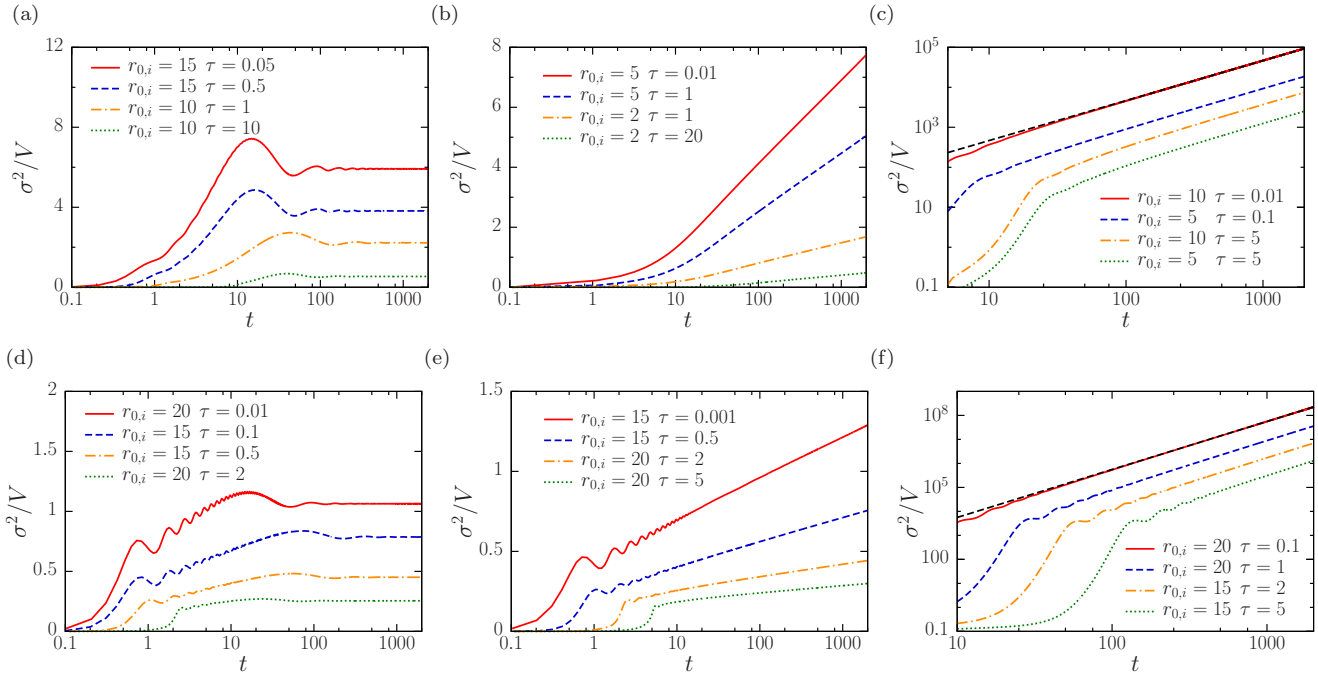

FIG. 8. Variance per unit volume for ramps above [(a) and (d)], at [(b) and (e)], and below [(c) and (f)] the dynamical critical point in $d = 3$ (first row) and $d = 4$ (second row). Different values of the initial bare mass $r_{0,i}$ and of the ramp duration τ are shown, while the interaction is $\lambda = 15$. Black dashed lines in (c) and (f) are proportional, respectively, to t and t^2.

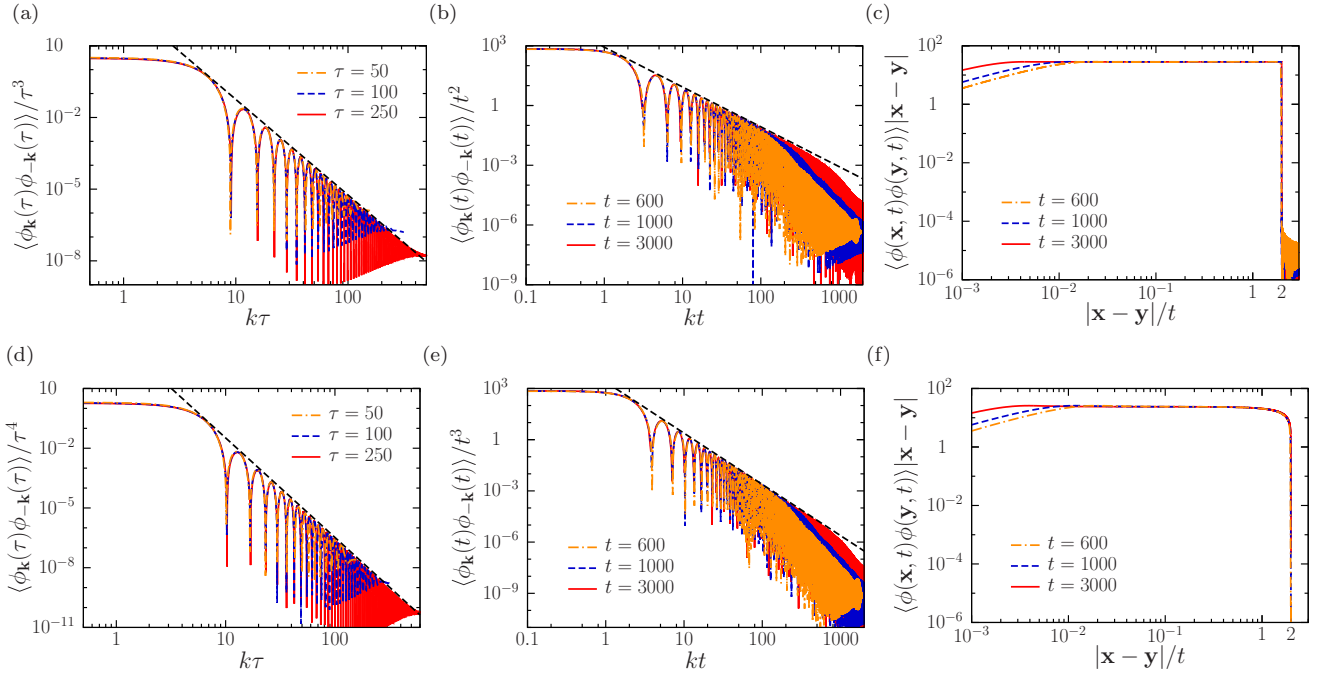

FIG. 9. Equal-time two-point correlation functions for ramps below the dynamical critical point in $d = 3$ (first row) and $d = 4$ (second row). In all the figures, the initial bare mass is $r_{0,i} = 15$, the final bare mass is $r_{0,f} = -15$, and the interaction is $\lambda = 15$. In (a) and (d) different values of the ramp duration τ are shown, and the black dashed lines are proportional, respectively, to $(k\tau)^{-4}$ and $(k\tau)^{-5}$. In (b) and (e) different values of the evolution time t are shown, for a ramp of duration $\tau = 20$, and the black dashed lines are proportional, respectively, to $(kt)^{-2}$ and $(kt)^{-3}$. In (c) and (f) different values of the evolution time t are shown, for a ramp of duration $\tau = 20$.

where $\mathcal{F}_d(k\tau)$ is an oscillating function decaying as $\sim(k\tau)^{-(d+1)}$ for $k\tau \gtrsim 1$.

In the subsequent evolution for $t > \tau$, shown in Figs. 9(b) and 9(e), the correlation function acquires a different dependence on momentum for $1/t \lesssim k \lesssim 1/\tau$, and, for long times after the end of the ramp, the scaling form found in the case of a sudden quench is recovered, namely

$$\langle \phi_{\mathbf{k}}(t)\phi_{-\mathbf{k}}(t)\rangle = t^{d-1}\mathcal{G}_d(kt), \tag{30}$$

where $\mathcal{G}_d(kt)$ is an oscillating function decaying as $\sim(kt)^{-(d-1)}$ for $1 \lesssim kt \lesssim t/\tau$. For $k \gtrsim 1/\tau$, instead, the correlation function still decays as $\sim k^{-(d+1)}$. Notice that in the limit $\tau \to 0$, the latter regime, which is due to the finite duration of the ramp, is suppressed.

The corresponding Fourier transform in real space, $\langle \phi(\mathbf{x},t)\phi(\mathbf{y},t)\rangle$, shown in Figs. 9(c) and 9(f), exhibits a light-cone structure [13,49,61], vanishing for $|\mathbf{x}-\mathbf{y}| > 2t$ as a consequence of the finite speed of propagation of excitations, and it decays as $|\mathbf{x}-\mathbf{y}|^{-1}$ for $\tau \lesssim |\mathbf{x}-\mathbf{y}| < 2t$, both in $d = 3$ and in $d = 4$. While in the limit $\tau \to 0$ the result of a sudden quench is fully recovered, for $\tau \to \infty$ we do not find the corresponding equilibrium correlation function, since the $O(N)$ symmetry cannot be globally broken by the dynamics. Moreover, adiabaticity is not expected to hold, since the system crosses the dynamical critical point and enters a gapless phase.

VI. CONCLUSIONS

In this work, we investigated the crossover of the dynamical phase transitions of the $O(N)$ vector model in the $N \to \infty$ limit as a function of the duration of a linear ramp in the bare mass. In particular, we have shown that, when the duration of the ramp is finite, the critical properties associated with dynamical transitions are the same as the equilibrium transition at finite temperature, while as $\tau \to +\infty$ they are close to those of the equilibrium system at zero temperature, i.e., the quantum phase transition. Studying in detail the value of the bare mass at the dynamical critical point $r^c_{0,f}(\tau)$, we investigated how its value interpolates between the limiting cases of the sudden quench ($\tau \to 0$) and the adiabatic switching ($\tau \to \infty$) of the bare mass. We found that the approach to these two limits is algebraic in τ, and we derived analytically the values of such exponents.

As for a sudden quench, the nonequilibrium nature of the dynamical transition, however, leaves strong signatures on the statistics of the excitations, whose variance grows as a power law below the critical point and exhibits a logarithmic behavior at the critical point. An intriguing crossover is finally observed analyzing the equal-time two-point correlation function for ramps below the dynamical critical point. There we found the emergence of two different scaling behaviors, one related to the finite duration of the ramp (unrelated to quantum critical scaling) and the other to the subsequent time evolution and coarsening dynamics.

APPENDIX A: NONINTERACTING THEORY AND STATIONARY VALUES

In this appendix, we explicitly solve Eqs. (8) in the case of a free theory, i.e., $\lambda = 0$, and we provide additional details on the ansatz of Eq. (9).

Obviously, when $\lambda = 0$ the effective mass is equal to the bare one, therefore we have to solve the equation

$$\ddot{f}^0_k(t) + [k^2 + r_0(t)]f^0_k(t) = 0 \tag{A1}$$

with the initial conditions $f^0_k(0) = 1/[4(k^2+r_{0,i})]^{1/4}$ and $\dot{f}^0_k(0) = -i[(k^2+r_{0,i})/4]^{1/4}$.

For $0 < t < \tau$, the solution is given by

$$\begin{aligned} f^0_k(t) = {} & \frac{\pi}{\sqrt{2}(k^2+r_{0,i})^{1/4}}\left[\mathrm{Ai}\left(\gamma t - \frac{k^2+r_{0,i}}{\gamma^2}\right)\mathrm{Bi}'\left(-\frac{k^2+r_{0,i}}{\gamma^2}\right) - \mathrm{Ai}'\left(-\frac{k^2+r_{0,i}}{\gamma^2}\right)\mathrm{Bi}\left(\gamma t - \frac{k^2+r_{0,i}}{\gamma^2}\right)\right] \\ & + \frac{i\pi(k^2+r_{0,i})^{1/4}}{\sqrt{2}\gamma}\left[\mathrm{Ai}\left(\gamma t - \frac{k^2+r_{0,i}}{\gamma^2}\right)\mathrm{Bi}\left(-\frac{k^2+r_{0,i}}{\gamma^2}\right) - \mathrm{Ai}\left(-\frac{k^2+r_{0,i}}{\gamma^2}\right)\mathrm{Bi}\left(\gamma t - \frac{k^2+r_{0,i}}{\gamma^2}\right)\right], \end{aligned} \tag{A2}$$

where $\gamma = [(r_{0,i} - r_{0,f})/\tau]^{1/3}$, and $\mathrm{Ai}(x)$ and $\mathrm{Bi}(x)$ denote the Airy functions, while for $t > \tau$

$$f^0_k(t) = f^0_k(\tau)\cos\left(\sqrt{k^2+r_{0,f}}(t-\tau)\right) + \frac{\dot{f}^0_k(\tau)}{\sqrt{k^2+r_{0,f}}}\sin\left(\sqrt{k^2+r_{0,f}}(t-\tau)\right), \tag{A3}$$

where $f^0_k(\tau)$ and $\dot{f}^0_k(\tau)$ have to be read from Eq. (A2).

Using Eqs. (A2) and (A3), we can explicitly compute the two-body equal-time Green's function $\langle \phi_{\mathbf{k}}(t)\phi_{-\mathbf{k}}(t)\rangle = |f^0_k(t)|^2$, which, for $t > \tau$, is

$$\begin{aligned} \langle \phi_{\mathbf{k}}(t)\phi_{-\mathbf{k}}(t)\rangle = {} & \frac{1}{2}\Bigg[|f^0_k(\tau)|^2 + \frac{|\dot{f}^0_k(\tau)|^2}{k^2+r_{0,f}} + \left(|f^0_k(\tau)|^2 - \frac{|\dot{f}^0_k(\tau)|^2}{k^2+r_{0,f}}\right)\cos\left(\sqrt{k^2+r_{0,f}}(t-\tau)\right) \\ & + \frac{2\,\mathrm{Re}\left(f^0_k(\tau)\dot{f}^{0\star}_k(\tau)\right)}{\sqrt{k^2+r_{0,f}}}\sin\left(\sqrt{k^2+r_{0,f}}(t-\tau)\right)\Bigg]. \end{aligned} \tag{A4}$$

When $\lambda \neq 0$, we have to resort to numerical integration of Eqs. (8), which shows that for long times after the end of the ramp the effective mass $r(t)$ relaxes to a stationary value. To predict the stationary value r^*, we use the following ansatz: after the end

of the ramp, we assume the stationary part of the two-body equal-time Green's function to be equal to the noninteracting one, but with the bare masses and the ramp duration replaced by the renormalized ones. Namely, we take Eq. (A4), disregard all the oscillatory terms, and replace $r_{0,i} \to r_i$, $r_{0,f} \to r^*$, and $\tau \to \tilde{\tau}$. Thus, we obtain the following self-consistent equation for r^*:

$$r^* = r_{0,f} + \frac{\lambda}{12}\int^{\Lambda} \frac{d^d k}{(2\pi)^d}\left[\left|f_k^0(r^*,\tilde{\tau})\right|^2 + \frac{\left|\dot{f}_k^0(r^*,\tilde{\tau})\right|^2}{k^2+r^*}\right], \tag{A5}$$

where

$$f_k^0(r^*,\tilde{\tau}) = \frac{\pi}{\sqrt{2}(k^2+r_i)^{1/4}}\left[\mathrm{Ai}\left(-\frac{k^2+r^*}{\tilde{\gamma}^2}\right)\mathrm{Bi}'\left(-\frac{k^2+r_i}{\tilde{\gamma}^2}\right) - \mathrm{Ai}'\left(-\frac{k^2+r_i}{\tilde{\gamma}^2}\right)\mathrm{Bi}\left(-\frac{k^2+r^*}{\tilde{\gamma}^2}\right)\right]$$
$$+ \frac{i\pi(k^2+r_i)^{1/4}}{\sqrt{2}\tilde{\gamma}}\left[\mathrm{Ai}\left(-\frac{k^2+r^*}{\tilde{\gamma}^2}\right)\mathrm{Bi}\left(-\frac{k^2+r_i}{\tilde{\gamma}^2}\right) - \mathrm{Ai}\left(-\frac{k^2+r_i}{\tilde{\gamma}^2}\right)\mathrm{Bi}\left(-\frac{k^2+r^*}{\tilde{\gamma}^2}\right)\right], \tag{A6}$$

$$\dot{f}_k^0(r^*,\tilde{\tau}) = \frac{\pi\tilde{\gamma}}{\sqrt{2}(k^2+r_i)^{1/4}}\left[\mathrm{Ai}'\left(-\frac{k^2+r^*}{\tilde{\gamma}^2}\right)\mathrm{Bi}'\left(-\frac{k^2+r_i}{\tilde{\gamma}^2}\right) - \mathrm{Ai}'\left(-\frac{k^2+r_i}{\tilde{\gamma}^2}\right)\mathrm{Bi}'\left(-\frac{k^2+r^*}{\tilde{\gamma}^2}\right)\right]$$
$$+ \frac{i\pi(k^2+r_i)^{1/4}}{\sqrt{2}}\left[\mathrm{Ai}'\left(-\frac{k^2+r^*}{\tilde{\gamma}^2}\right)\mathrm{Bi}\left(-\frac{k^2+r_i}{\tilde{\gamma}^2}\right) - \mathrm{Ai}\left(-\frac{k^2+r_i}{\tilde{\gamma}^2}\right)\mathrm{Bi}'\left(-\frac{k^2+r^*}{\tilde{\gamma}^2}\right)\right], \tag{A7}$$

with $\tilde{\gamma} = ((r_i - r^*)/\tilde{\tau})^{1/3}$.

APPENDIX B: DYNAMICAL CRITICAL PROPERTIES

In this appendix, we provide the detailed computation of the critical dimensions and critical exponent ν^*.

For studying the lower critical dimension, it is useful to recall the expansions of the Airy functions both for small and large arguments [62]. For small x, we have

$$\mathrm{Ai}(-x) = \frac{1}{3^{2/3}\Gamma(2/3)} + \frac{x}{3^{1/3}\Gamma(1/3)} + O(x^3), \tag{B1a}$$

$$\mathrm{Ai}'(-x) = -\frac{1}{3^{1/3}\Gamma(1/3)} + \frac{x^2}{2\cdot 3^{2/3}\Gamma(2/3)} + O(x^3), \tag{B1b}$$

$$\mathrm{Bi}(-x) = \frac{1}{3^{1/6}\Gamma(2/3)} - \frac{3^{1/6}x}{\Gamma(1/3)} + O(x^3), \tag{B1c}$$

$$\mathrm{Bi}'(-x) = \frac{3^{1/6}}{\Gamma(1/3)} + \frac{x^2}{2\cdot 3^{1/6}\Gamma(2/3)} + O(x^3), \tag{B1d}$$

while for large and positive x we have

$$\mathrm{Ai}(-x) = \frac{1}{\sqrt{\pi}x^{1/4}}\sin\left(\frac{\pi}{4} + \frac{2}{3}x^{3/2}\right) + O(x^{-7/4}), \tag{B2a}$$

$$\mathrm{Ai}'(-x) = -\frac{x^{1/4}}{\sqrt{\pi}}\cos\left(\frac{\pi}{4} + \frac{2}{3}x^{3/2}\right) + O(x^{-5/4}), \tag{B2b}$$

$$\mathrm{Bi}(-x) = \frac{1}{\sqrt{\pi}x^{1/4}}\cos\left(\frac{\pi}{4} + \frac{2}{3}x^{3/2}\right) + O(x^{-7/4}), \tag{B2c}$$

$$\mathrm{Bi}'(-x) = \frac{x^{1/4}}{\sqrt{\pi}}\sin\left(\frac{\pi}{4} + \frac{2}{3}x^{3/2}\right) + O(x^{-5/4}). \tag{B2d}$$

We can now analyze the behavior for low momenta of the integrand of Eq. (A5) with $r^* = 0$. For every finite τ, the most relevant modes are those with $k \ll (r_i/\tilde{\tau})^{1/3}$ and $k \ll \sqrt{r_i}$. In this region and for $r^* = 0$, we can replace all the Airy functions with the argument $-(k^2+r^*)/\tilde{\gamma}^2$ with their zero value [see Eqs. (B1)], while the leading order of all the other terms is obtained setting $k = 0$. Thus, we conclude that both $f_k^0(0,\tilde{\tau})$ and $\dot{f}_k^0(0,\tilde{\tau})$ are constant in k. As a consequence, the lower critical dimension for every finite τ is $d = 2$. Instead, to understand what happens in the limit $\tau \to \infty$, we have to take into account the region $(r_i/\tilde{\tau})^{1/3} \ll k \ll \sqrt{r_i}$. Here, and for $r^* = 0$, we have to substitute the Airy functions with the argument $-(k^2+r^*)/\tilde{\gamma}^2$ with their asymptotic expansions of Eqs. (B2), and set $k = 0$ in all the other terms. Thus, we see that $f_k^0(0,\tilde{\tau}) \sim 1/\sqrt{k}$ and $\dot{f}_k^0(0,\tilde{\tau}) \sim \sqrt{k}$. So, when τ is strictly infinite, the lower critical dimension is $d = 1$.

To determine the critical exponent ν^*, we analyze the behavior of the asymptotic mass r^* for small distances of $r_{0,f}$ from the dynamical critical point. Denoting $\delta r_{0,f}(\tau) = r_{0,f} - r_{0,f}^c(\tau)$, defining the dimensionless variable $\mathbf{y} = \mathbf{k}/\sqrt{r^*}$, and combining Eqs. (9) and (10), we can write

$$r^* = \delta r_{0,f}(\tau) + \frac{\lambda}{12}(r^*)^{\frac{d-2}{2}}\int^{\Lambda/\sqrt{r^*}} \frac{d^d y}{(2\pi)^d} \times \frac{y^2 g(y\sqrt{r^*},r^*) - (y^2+1)g(y\sqrt{r^*},0)}{y^2(y^2+1)}, \tag{B3}$$

with

$$g(k,r^*) = \left|f_k^0(r^*,\tilde{\tau})\right|^2(k^2+r^*) + \left|\dot{f}_k^0(r^*,\tilde{\tau})\right|^2. \tag{B4}$$

The asymptotic behavior of the integral in Eq. (B3) for small r^* is determined by the behavior of the integrand in the region $1 \ll y \ll \sqrt{r_i/r^*}$, where it scales as $g(0,0)/y^4$. Thus, for $2 < d < 4$ the dominant contribution to the integral in powers of r^* is obtained by replacing the upper limit of integration with infinity and the integrand with its leading order in r^*, namely

$$r^* \simeq \delta r_{0,f}(\tau) - \frac{\lambda}{12}\frac{\Omega(d)}{(2\pi)^d}(r^*)^{\frac{d-2}{2}}\int_0^\infty dy\, y^{d-1}\frac{g(0,0)}{y^2(y^2+1)}$$
$$= \delta r_{0,f}(\tau) + \frac{\lambda}{12}\frac{\Omega(d)}{(2\pi)^d}(r^*)^{\frac{d-2}{2}}\frac{\pi\, g(0,0)}{2\sin(d\pi/2)}, \tag{B5}$$

where $\Omega(d)$ is the solid angle. So, we conclude that at the leading order $r^* \sim [\delta r_{0,f}(\tau)]^{\frac{2}{d-2}}$. For $d = 4$ we have logarithmic corrections to this scaling, while for $d > 4$ the divergence of the integral can be deduced by considering

the scaling of the integrand mentioned above. We have that the integral diverges as $(r^*)^{-\frac{d-4}{2}}$, giving a linear relation $r^* \sim \delta r_{0,f}(\tau)$ at the leading order. Therefore, we can recover the values of Eq. (21) for the critical exponent ν^*.

APPENDIX C: ASYMPTOTIC EXPANSIONS FOR LARGE τ

In this appendix, we provide additional details on the derivation of Eqs. (16) and (17). Let us start by considering the case of $d = 3$. Computing the integrals (15), we obtain

$$\mathcal{I}_1(3) = \Lambda^2\Bigg[\frac{2\pi}{3^{1/3}\Gamma^2(-1/3)}\,{}_2F_3\left(\frac{1}{6},\frac{1}{2};\frac{1}{3},\frac{2}{3},\frac{3}{2};-\frac{4}{9}y^2\right)y^{1/3} - \frac{1}{5\sqrt{3}}\,{}_2F_3\left(\frac{1}{2},\frac{5}{6};\frac{2}{3},\frac{4}{3},\frac{11}{6};-\frac{4}{9}y^2\right)y + \frac{\Gamma(5/6)}{2^{1/3}\cdot 3^{1/6}\cdot 7\sqrt{\pi}}\,{}_2F_3\left(\frac{5}{6},\frac{7}{6};\frac{4}{3},\frac{5}{3},\frac{13}{6};-\frac{4}{9}y^2\right)y^{5/3}\Bigg], \tag{C1a}$$

$$\mathcal{I}_2(3) = \Lambda^2\Bigg[-\frac{3^{1/3}\Gamma(-1/3)\Gamma(5/3)}{4\pi}\,{}_2F_3\left(-\frac{1}{6},\frac{1}{6};-\frac{1}{3},\frac{1}{3},\frac{7}{6};-\frac{4}{9}y^2\right)y^{-1/3} + \frac{1}{10\sqrt{3}}\,{}_2F_3\left(\frac{1}{2},\frac{5}{6};\frac{1}{3},\frac{5}{3},\frac{11}{6};-\frac{4}{9}y^2\right)y + \frac{\Gamma(1/6)}{2^{2/3}\cdot 3^{5/6}\cdot 36\sqrt{\pi}}\,{}_2F_3\left(\frac{7}{6},\frac{3}{2};\frac{5}{3},\frac{7}{3},\frac{5}{2};-\frac{4}{9}y^2\right)y^{7/3}\Bigg], \tag{C1b}$$

where ${}_2F_3(a,b;c,d,e;x)$ denotes the hypergeometric function and $y = \Lambda^3\tilde{\tau}/r_i$. Taking the asymptotic expansions of the hypergeometric functions for large y, namely

$${}_2F_3\left(\frac{1}{6},\frac{1}{2};\frac{1}{3},\frac{2}{3},\frac{3}{2};-\frac{4}{9}y^2\right) = \frac{3^{5/6}\sqrt{\pi}}{2^{1/3}\Gamma(1/6)}\,y^{-1/3} - \frac{\sqrt{3\pi}\,\Gamma(-1/3)}{24\,\Gamma(1/6)}\,y^{-1} + O(y^{-5/3}), \tag{C2a}$$

$${}_2F_3\left(\frac{1}{2},\frac{5}{6};\frac{2}{3},\frac{4}{3},\frac{11}{6};-\frac{4}{9}y^2\right) = \frac{5}{4\sqrt{3}}\,y^{-1} - \frac{5\,\Gamma(-1/3)}{2^{8/3}\times 3^{11/6}}\,y^{-5/3} + O(y^{-7/3}), \tag{C2b}$$

$${}_2F_3\left(\frac{5}{6},\frac{7}{6};\frac{4}{3},\frac{5}{3},\frac{13}{6};-\frac{4}{9}y^2\right) = \frac{7\sqrt{\pi}}{2^{2/3}\times 3^{5/6}\Gamma(5/6)}\,y^{-5/3} + \frac{7\sqrt{\pi}\,\Gamma(-1/3)}{2^{7/3}\times 3^{13/6}\Gamma(5/6)}\,y^{-7/3} + O(y^{-3}), \tag{C2c}$$

$${}_2F_3\left(-\frac{1}{6},\frac{1}{6};-\frac{1}{3},\frac{1}{3},\frac{7}{6};-\frac{4}{9}y^2\right) = \frac{\Gamma(4/3)}{3^{5/6}\Gamma(5/3)}\,y^{1/3} + \frac{\pi}{2^{2/3}\times 3^{5/3}\Gamma(5/3)}\,y^{-1/3} + O(y^{-1}), \tag{C2d}$$

$${}_2F_3\left(\frac{1}{2},\frac{5}{6};\frac{1}{3},\frac{5}{3},\frac{11}{6};-\frac{4}{9}y^2\right) = -\frac{5}{2\sqrt{3}}\,y^{-1} - \frac{5\,\Gamma(-1/3)}{2^{5/3}\times 3^{5/6}}\,y^{-5/3} + O(y^{-7/3}), \tag{C2e}$$

$${}_2F_3\left(\frac{7}{6},\frac{3}{2};\frac{5}{3},\frac{7}{3},\frac{5}{2};-\frac{4}{9}y^2\right) = \frac{2^{2/3}\times 3^{5/6}\times 6\sqrt{\pi}}{\Gamma(1/6)}\,y^{-7/3} - \frac{27\sqrt{3\pi}\,\Gamma(5/3)}{4\,\Gamma(1/6)}\,y^{-3} + O(y^{-11/3}), \tag{C2f}$$

we get

$$\mathcal{I}_1(3) = \frac{\Lambda^2}{4} + \frac{\Gamma(-1/3)}{2^{11/3}\times 3^{4/3}}\left(\frac{r_i}{\tilde{\tau}}\right)^{2/3} + O\left(\frac{r_i^{4/3}}{\Lambda^4\tilde{\tau}^{4/3}}\right), \tag{C3a}$$

$$\mathcal{I}_2(3) = \frac{\Lambda^2}{4} - \frac{\Gamma(-1/3)}{2^{11/3}\times 3^{1/3}}\left(\frac{r_i}{\tilde{\tau}}\right)^{2/3} + O\left(\frac{r_i^{4/3}}{\Lambda^4\tilde{\tau}^{4/3}}\right). \tag{C3b}$$

Using these results, we can recover Eq. (16).

For $d = 4$, we have

$$\mathcal{I}_1(4) + \mathcal{I}_2(4) = \Lambda^3\Bigg\{\frac{1}{12\sqrt{3}}\,y^{-1} + \frac{\pi}{12}\{2y^{1/3}[\mathrm{Ai}'^2(-y^{2/3}) + \mathrm{Bi}'^2(-y^{2/3})] + 2y^{-1/3}[\mathrm{Ai}^2(-y^{2/3}) + \mathrm{Bi}^2(-y^{2/3})] - y^{-1}[\mathrm{Ai}(-y^{2/3})\mathrm{Ai}'(-y^{2/3}) + \mathrm{Bi}(-y^{2/3})\mathrm{Bi}'(-y^{2/3})]\}\Bigg\}, \tag{C4}$$

where we introduced $y = \Lambda^3\tilde{\tau}/r_i$. Expanding the Airy functions for large and negative arguments, we finally obtain

$$\mathcal{I}_1(4) + \mathcal{I}_2(4) = -\frac{\Lambda^3}{3} + \frac{1}{12\sqrt{3}}\left(\frac{r_i}{\tilde{\tau}}\right) + O\left(\frac{r_i^2}{\Lambda^6\tilde{\tau}^2}\right), \tag{C5}$$

from which Eq. (17) follows.

APPENDIX D: MOMENT-GENERATING FUNCTION

In this appendix, we derive the moment-generating function, defined as

$$G(s,t) = \langle\psi(t)|\, e^{-s\hat{\mathcal{N}}}\, |\psi(t)\rangle, \tag{D1}$$

where $\hat{\mathcal{N}}$ is the operator describing the number of excitations, $|\psi(t)\rangle = U(t)|0\rangle$ is the evolved state at time t, and $|0\rangle$ indicates the initial ground state.

Since the effective theory is quadratic and different k-modes are coupled only via $r(t)$, the moment-generating function can be factorized as

$$G(s,t) = \prod_k G_k(s,t), \tag{D2}$$

where $G_k(s,t)$ is the moment-generating function for a single k-mode.

To compute $G_k(s,t)$, we have to write the evolved state $|\psi(t)\rangle$ in terms of the operators $a_{\mathbf{k}}$ and $a^\dagger_{\mathbf{k}}$ diagonalizing the initial Hamiltonian. Toward that end, we introduce a time-dependent operator $\tilde{a}_{\mathbf{k}}(t)$ such that $\tilde{a}_{\mathbf{k}}(t)|\psi(t)\rangle = 0$. Since $a_{\mathbf{k}} = U^\dagger(t)\tilde{a}_{\mathbf{k}}(t)U(t)$, using Eq. (7), we have that

$$\phi_{\mathbf{k}}(0) = f_k(t)\tilde{a}_{\mathbf{k}}(t) + f_k^\star(t)\tilde{a}^\dagger_{-\mathbf{k}}(t), \tag{D3a}$$

$$\Pi_{\mathbf{k}}(0) = \dot{f}_k(t)\tilde{a}_{\mathbf{k}}(t) + \dot{f}_k^\star(t)\tilde{a}^\dagger_{-\mathbf{k}}(t). \tag{D3b}$$

Furthermore, we know that at $t = 0$

$$\phi_{\mathbf{k}}(0) = \frac{1}{\sqrt{2\omega_k(0)}}(a_{\mathbf{k}} + a^\dagger_{-\mathbf{k}}), \tag{D4a}$$

$$\Pi_{\mathbf{k}}(0) = i\sqrt{\frac{\omega_k(0)}{2}}(a^\dagger_{-\mathbf{k}} - a_{\mathbf{k}}). \tag{D4b}$$

Combining Eqs. (D3) and (D4), and using the fact that $f_k(t)\dot{f}_k^\star(t) - f_k^\star(t)\dot{f}_k(t) = i$, we get

$$\tilde{a}_{\mathbf{k}}(t) = \alpha_k^\star(t)a_{\mathbf{k}} - \beta_k^\star(t)a^\dagger_{-\mathbf{k}}, \tag{D5}$$

with

$$\alpha_k(t) = \sqrt{\frac{\omega_k(0)}{2}}f_k(t) + \frac{i}{\sqrt{2\omega_k(0)}}\dot{f}_k(t), \tag{D6a}$$

$$\beta_k(t) = \sqrt{\frac{\omega_k(0)}{2}}f_k(t) - \frac{i}{\sqrt{2\omega_k(0)}}\dot{f}_k(t). \tag{D6b}$$

Since the evolved state must be annihilated by the operator $\tilde{a}_{\mathbf{k}}(t)$ of Eq. (D5), we finally obtain

$$|\psi(t)\rangle_k = \frac{1}{\sqrt{|\alpha_k(t)|}}\exp\left(\frac{\beta_k^\star(t)}{2\alpha_k^\star(t)}a^\dagger_{\mathbf{k}}a^\dagger_{-\mathbf{k}}\right)|0\rangle, \tag{D7}$$

with $a_{\mathbf{k}}\,|\,0\rangle = 0$.

Now we can readily compute the moment-generating function for a single k-mode, that is,

$$G_k(s,t) = \frac{1}{\sqrt{1+\rho_k(t)(1-e^{-2s})}}, \tag{D8}$$

where

$$\rho_k(t) = |\beta_k(t)|^2 = \frac{1}{2}\left(\omega_k(0)|f_k(t)|^2 + \frac{|\dot{f}_k(t)|^2}{\omega_k(0)} - 1\right). \tag{D9}$$

Using the relation

$$\ln G(s,t) = L^d\int^\Lambda \frac{d^dk}{(2\pi)^d}\ln G_k(s,t), \tag{D10}$$

we finally recover the result of Eq. (24).

[1] A. Polkovnikov, K. Sengupta, A. Silva, and M. Vengalattore, Rev. Mod. Phys. **83**, 863 (2011).

[2] A. Lamacraft and J. Moore, in *Ultracold Bosonic and Fermionic Gases*, edited by A. L. F. Kathryn Levin and D. M. Stamper-Kurn (Elsevier, Amsterdam, 2012), Vol. 5, Chap. 7, pp. 177–202.

[3] J. Dziarmaga, Adv. Phys. **59**, 1063 (2010).

[4] V. I. Yukalov, Laser Phys. Lett. **8**, 485 (2011).

[5] I. Bloch, J. Dalibard, and W. Zwerger, Rev. Mod. Phys. **80**, 885 (2008).

[6] M. Greiner, O. Mandel, T. Esslinger, T. W. Hänsch, and I. Bloch, Nature (London) **415**, 39 (2002).

[7] M. Greiner, O. Mandel, T. W. Hansch, and I. Bloch, Nature (London) **419**, 51 (2002).

[8] L. E. Sadler, J. M. Higbie, S. R. Leslie, M. Vengalattore, and D. M. Stamper-Kurn, Nature (London) **443**, 312 (2006).

[9] T. Kinoshita, T. Wenger, and D. S. Weiss, Nature (London) **440**, 900 (2006).

[10] T. Kitagawa, A. Imambekov, J. Schmiedmayer, and E. Demler, New J. Phys. **13**, 073018 (2011).

[11] M. Gring, M. Kuhnert, T. Langen, T. Kitagawa, B. Rauer, M. Schreitl, I. Mazets, D. A. Smith, E. Demler, and J. Schmiedmayer, Science **337**, 1318 (2012).

[12] T. Langen, R. Geiger, M. Kunhert, B. Rauer, and J. Schmiedmayer, Nat. Phys. **9**, 640 (2013).

[13] M. Cheneau, P. Barmettler, D. Poletti, M. Endres, P. Schaub, T. Fukuhara, C. Gross, I. Bloch, C. Kollath, and S. Kuhr, Nature (London) **481**, 484 (2012).

[14] J. M. Deutsch, Phys. Rev. A **43**, 2046 (1991).

[15] M. Srednicki, Phys. Rev. E **50**, 888 (1994).

[16] M. Rigol, V. Dunjko, and M. Olshanii, Nature (London) **452**, 854 (2008).

[17] M. Rigol, V. Dunjko, V. Yurovsky, and M. Olshanii, Phys. Rev. Lett. **98**, 050405 (2007).

[18] T. Barthel and U. Schollwöck, Phys. Rev. Lett. **100**, 100601 (2008).

[19] M. Kollar and M. Eckstein, Phys. Rev. A **78**, 013626 (2008).

[20] A. Iucci and M. A. Cazalilla, Phys. Rev. A **80**, 063619 (2009).

[21] M. A. Cazalilla, A. Iucci, and M.-C. Chung, Phys. Rev. E **85**, 011133 (2012).

[22] E. T. Jaynes, Phys. Rev. **106**, 620 (1957).
[23] J. Berges, S. Borsányi, and C. Wetterich, Phys. Rev. Lett. **93**, 142002 (2004).
[24] M. Moeckel and S. Kehrein, Phys. Rev. Lett. **100**, 175702 (2008).
[25] M. Moeckel and S. Kehrein, Ann. Phys. (NY) **324**, 2146 (2009).
[26] M. Moeckel and S. Kehrein, New J. Phys. **12**, 055016 (2010).
[27] M. Kollar, F. A. Wolf, and M. Eckstein, Phys. Rev. B **84**, 054304 (2011).
[28] J. Marino and A. Silva, Phys. Rev. B **86**, 060408 (2012).
[29] M. Marcuzzi, J. Marino, A. Gambassi, and A. Silva, Phys. Rev. Lett. **111**, 197203 (2013).
[30] F. H. L. Essler, S. Kehrein, S. R. Manmana, and N. J. Robinson, Phys. Rev. B **89**, 165104 (2014).
[31] M. van den Worm, B. C. Sawyer, J. J. Bollinger, and M. Kastner, New J. Phys. **15**, 083007 (2013).
[32] N. Nessi, A. Iucci, and M. A. Cazalilla, Phys. Rev. Lett. **113**, 210402 (2014).
[33] M. Fagotti, J. Stat. Mech. (2014) P03016.
[34] B. Bertini and M. Fagotti, J. Stat. Mech. (2015) P07012.
[35] B. Bertini, F. H. L. Essler, S. Groha, and N. J. Robinson, Phys. Rev. Lett. **115**, 180601 (2015).
[36] G. Menegoz and A. Silva, J. Stat. Mech. (2015) P05035.
[37] M. Fagotti and M. Collura, arXiv:1507.02678.
[38] M. Babadi, E. Demler, and M. Knap, Phys. Rev. X **5**, 041005 (2015).
[39] G. P. Brandino, J.-S. Caux, and R. M. Konik, Phys. Rev. X **5**, 041043 (2015).
[40] E. Kaminishi, T. Mori, T. N. Ikeda, and M. Ueda, Nat. Phys. **11**, 1050 (2015).
[41] M. Heyl, A. Polkovnikov, and S. Kehrein, Phys. Rev. Lett. **110**, 135704 (2013).
[42] B. Zunkovic, M. Heyl, M. Knap, and A. Silva, arXiv:1609.08482.
[43] M. Eckstein, M. Kollar, and P. Werner, Phys. Rev. Lett. **103**, 056403 (2009).
[44] M. Schiró and M. Fabrizio, Phys. Rev. Lett. **105**, 076401 (2010).
[45] N. Tsuji, M. Eckstein, and P. Werner, Phys. Rev. Lett. **110**, 136404 (2013).
[46] B. Sciolla and G. Biroli, Phys. Rev. Lett. **105**, 220401 (2010).
[47] B. Sciolla and G. Biroli, J. Stat. Mech: Theor. Expt. (2011) P11003.
[48] A. Gambassi and P. Calabrese, Europhys. Lett. **95**, 66007 (2011).
[49] B. Sciolla and G. Biroli, Phys. Rev. B **88**, 201110(R) (2013).
[50] P. Smacchia, M. Knap, E. Demler, and A. Silva, Phys. Rev. B **91**, 205136 (2015).
[51] A. Chiocchetta, M. Tavora, A. Gambassi, and A. Mitra, Phys. Rev. B **91**, 220302 (2015).
[52] M. Moshe and J. Zinn-Justin, Phys. Rep. **385**, 69 (2003).
[53] F. Cooper, S. Habib, Y. Kluger, E. Mottola, J. P. Paz, and P. R. Anderson, Phys. Rev. D **50**, 2848 (1994).
[54] F. Cooper, S. Habib, Y. Kluger, and E. Mottola, Phys. Rev. D **55**, 6471 (1997).
[55] D. Boyanovsky, H. J. de Vega, R. Holman, and J. F. J. Salgado, Phys. Rev. D **54**, 7570 (1996).
[56] D. Boyanovsky, H. J. de Vega, R. Holman, and J. Salgado, Phys. Rev. D **59**, 125009 (1999).
[57] A. Maraga, A. Chiocchetta, A. Mitra, and A. Gambassi, Phys. Rev. E **92**, 042151 (2015).
[58] S. Sotiriadis and J. Cardy, Phys. Rev. B **81**, 134305 (2010).
[59] A. Chandran, A. Nanduri, S. S. Gubser, and S. L. Sondhi, Phys. Rev. B **88**, 024306 (2013).
[60] R. Botet and R. Jullien, Phys. Rev. B **28**, 3955 (1983).
[61] P. Calabrese and J. Cardy, J. Stat. Mech. (2007) P06008.
[62] M. Abramowitz and I. Stegun, *Handbook of Mathematical Functions: With Formulas, Graphs, and Mathematical Tables* (Dover, Mineola, NY, 1964).